Neuron 52, 1011–1025, December 21, 2006 ©2006 Elsevier Inc. DOI 10.1016/j.neuron.2006.10.020

The Adhesion Molecule CHL1 Regulates Uncoating of Clathrin-Coated Synaptic Vesicles

Iryna Leshchyns'ka,[1,3] Vladimir Sytnyk,[1,3] Melanie Richter,[1,3,4] Aksana Andreyeva,[1] Dmytro Puchkov,[1] and Melitta Schachner[1,2,*]
[1] Zentrum für Molekulare Neurobiologie
Universität Hamburg
Martinistrasse 52
20246 Hamburg
Germany
[2] Keck Center for Collaborative Neuroscience
Rutgers University
604 Allison Road
Piscataway, New Jersey 08854

Summary

In searching for binding partners of the intracellular domain of the immunoglobulin superfamily adhesion molecule CHL1, we identified the clathrin-uncoating ATPase Hsc70. CHL1 gene ablation resulted in reduced targeting of Hsc70 to the synaptic plasma membrane and synaptic vesicles, suggesting CHL1 as a synapse-targeting cue for Hsc70. CHL1 accumulates in presynaptic membranes and, in response to synapse activation, is targeted to synaptic vesicles by endocytosis. CHL1 deficiency or disruption of the CHL1/Hsc70 complex results in accumulation of abnormally high levels of clathrin-coated synaptic vesicles with a reduced ability to release clathrin. Generation of new clathrin-coated synaptic vesicles in an activity-dependent manner is inhibited when the CHL1/Hsc70 complex is disrupted, resulting in impaired uptake and release of FM dyes in synaptic boutons. Abnormalities in clathrin-dependent synaptic vesicle recycling may thus underlie brain malfunctions in humans and mice that carry mutations in the CHL1 gene.

Introduction

The close homolog of L1 (CHL1, also referred to as *CALL*) is a cell adhesion molecule of the immunoglobulin (Ig) superfamily. In the developing brain, CHL1 regulates neuronal migration (Buhusi et al., 2003) and neurite outgrowth (Hillenbrand et al., 1999). Mice deficient in CHL1 show reduced migration and positioning of pyramidal cells and elaboration of dendrites in the caudal, but not in the rostral, part of the cerebral cortex (Demyanenko et al., 2004). Mapping to chromosome h3p26.1 in humans, the CHL1 gene, may be associated with intelligence (Angeloni et al., 1999a). Loss or mutations of CHL1 may contribute to mental impairment associated with "3p-syndrome" (Angeloni et al., 1999b) and mental retardation (Frints et al., 2003). Ablation of the CHL1 gene in mice alters their exploratory behavior in a novel environment and reduces emotional reactivity and motor coordination (Montag-Sallaz et al., 2002; Pratte et al., 2003); CHL1 deficiency in mice leads to reduced prepulse inhibition of the acoustic startle response, a measure of the ability of the central nervous system to gate the flow of sensorimotor information (Irintchev et al., 2004). Mutations in CHL1 in humans correlate with the occurrence of schizophrenia (Sakurai et al., 2002; Chen et al., 2005), a neuropsychiatric disorder associated with abnormal neurocircuits and functioning of synapses (Harrison and Weinberger, 2005). Although these findings suggest that CHL1 regulates synapse functioning, the role of CHL1 in the organization of the synaptic machinery has not been fully analyzed.

The 70 kDa heat shock cognate protein (Hsc70) is a constitutively expressed member of the heat shock-inducible Hsp70 protein family. These proteins possess ATPase activity and perform numerous functions in cells, among which are protein folding and sorting, signal transduction, and apoptosis. Hsc70 also catalyzes, in vitro and in vivo, the release of clathrin from clathrin-coated vesicles as the final step of receptor-mediated endocytosis (Newmyer and Schmid, 2001). A similar function is attributed to Hsc70 in synapses, where Hsc70 regulates uncoating of synaptic vesicles (SVs) in the clathrin-dependent recycling pathway (Zinsmaier and Bronk, 2001). In this pathway, following SV fusion, the SV membrane is endocytosed via formation of clathrin-coated pits on the synaptic plasma membrane, resulting in formation of clathrin-coated synaptic vesicles (CCSVs) (Takei et al., 1996; Shupliakov et al., 1997).

During CCSV uncoating, Hsc70 co-operates with other proteins that target or regulate the activity of Hsc70, such as auxilin, which binds to Hsc70 in the presence of ATP and increases the activity of Hsc70 in CCSV uncoating (Morgan et al., 2001). In the present study, we show that Hsc70 binds to the intracellular domain of CHL1 and that this interaction is potentiated by ADP. CHL1 accumulates in the presynaptic plasma membrane, and there it recruits Hsc70 in an ADP-dependent manner. In response to synapse activation, CHL1 is targeted to SVs by endocytosis. CHL1 deficiency causes a reduction in levels of Hsc70 on SVs and leads to reduced clathrin release from CCSVs and reduced uptake and release of FM dyes in synaptic boutons. These observations suggest a role for CHL1 in regulating SV recycling via a clathrin-dependent pathway.

Results

Hsc70 Binds to the Intracellular Domain of CHL1

To identify binding partners of the CHL1 intracellular domain (CHL1-ID), soluble protein fraction from adult mouse brain was used for two-dimensional (2D) gel electrophoresis, after which proteins were either transferred to nitrocellulose membrane or subjected to silver staining. Blotted membranes were then incubated with recombinant CHL1-ID, and binding of CHL1-ID to proteins immobilized in the nitrocellulose membrane was analyzed. The most prominent binding was observed

*Correspondence: melitta.schachner@zmnh.uni-hamburg.de
[3] These authors contributed equally to this work.
[4] Present address: Pasquale lab, The Burnham Institute, 10901 North Torrey Pines Road, La Jolla, California 92037.

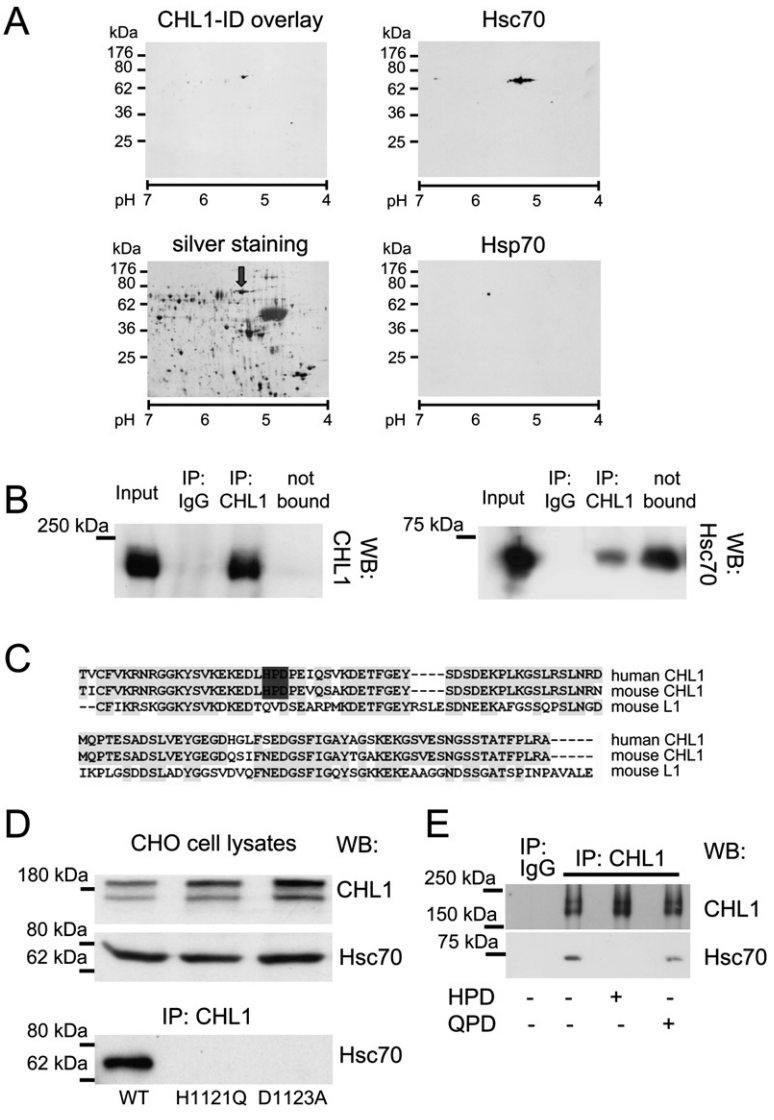

Figure 1. CHL1-ID Directly Interacts with Hsc70 via Its HPD Tripeptide

(A) A soluble fraction from adult mouse brain homogenate was separated by two-dimensional (2D) gel electrophoresis. Proteins were then transferred to nitrocellulose and subjected to an overlay assay with CHL1-ID. Alternatively, gels were silver stained. Note that CHL1-ID bound most prominently to a 70 kDa spot with the slightly acidic isoelectric point of 5.5. The dark gray arrow on the silver-stained gel shows the corresponding 70 kDa spot isolated and used for MALDI-MS analysis, which showed it to contain Hsc70. Stripped after the overlay, membranes were reprobed with antibodies against Hsc70 or Hsp70. Note that Hsc70 antibodies detected a spot overlapping with the area containing the binding partner of CHL1-ID. Antibodies against Hsp70 labeled a 70 kDa spot with the more basic 5.8 isoelectric point.

(B) CHL1 was immunoprecipitated (IP) from lysates of brain homogenates. Immunoprecipitates, protein input, and material not bound to the beads were probed with antibodies against CHL1 and Hsc70 by western blot (WB). Hsc70 was coimmunoprecipitated with CHL1. Immunoprecipitation with nonspecific immunoglobulins (IgG) was performed for control.

(C) Amino acid sequences of the IDs of human and mouse CHL1 and mouse L1 are shown. The HPD tripeptide is marked in dark gray in the IDs of human and mouse CHL1. Overlapping sequences are given in gray.

(D) CHO cells were transfected with full-length, wild-type mouse CHL1 (WT) or CHL1 containing the indicated mutations in the HPD tripeptide. The three CHL1 constructs and endogenous Hsc70 were expressed at similar levels in the cell lysates. Wild-type CHL1 and CHL1 mutants were IP from cell lysates. Hsc70 coimmunoprecipitated only with wild-type CHL1.

(E) Brain lysates were preincubated with the HPD tripeptide-containing peptide VKEKED LHPDPEVQSAKDET derived from CHL1-ID (HPD), or with a similar peptide VKEKEDLQPDPEVQSAKDET containing a point mutation in the HPD tripeptide (QPD). Whereas similar levels of CHL1 were IP, coimmunoprecipitation of Hsc70 was inhibited in lysates preincubated with the HPD tripeptide-containing peptide. Immunoprecipitation with nonspecific IgG was performed for control.

in the 70 kDa area at a slightly acidic isoelectric point of approximately 5.5 (Figure 1A). The corresponding spot in silver-stained gels was isolated and subjected to matrix-assisted laser desorption/ionization mass spectrometry (MALDI-MS) analysis, which identified heat shock cognate Hsc70. To confirm this finding, nitrocellulose membranes used for the overlay experiments were stripped and reprobed with antibodies against Hsc70, which indeed bound to the area overlapping with the spot containing the binding partner of CHL1-ID (Figure 1A). For comparison, antibodies against Hsp70 were used, which revealed a 70 kDa spot with the more basic isoelectric point of 5.8.

To analyze whether CHL1 associates with Hsc70 in brain tissue of adult mice, CHL1 was immunoprecipitated from brain lysates and immunoprecipitates were probed with antibodies against Hsc70. Approximately 20% of all Hsc70 coimmunoprecipitated with CHL1, suggesting that the observed interaction is physiologically relevant (Figure 1B).

Hsc70 Binds to the HPD Tripeptide in the Intracellular Domain of CHL1

Analysis of the CHL1-ID amino acid sequence revealed an HPD tripeptide that had been identified in other proteins as a binding site for Hsp70 proteins (Figure 1C). This conserved HPD motif is present in the J domains of DnaJ-like proteins, which are co-chaperones of Hsp70 proteins that bind to Hsp70 proteins to induce their ATPase activity. A single mutation of any amino acid in the HPD tripeptide blocks the interaction between DnaJ and Hsp70 proteins, indicating that the HPD motif is crucial for this interaction (Tsai and Douglas, 1996; Chamberlain and Burgoyne, 1997). Both mouse and human CHL1 sequences contain the HPD tripeptide, whereas it is not present in the intracellular domain of L1. To analyze the role of the HPD tripeptide in CHL1/Hsc70 complex formation, wild-type full-length CHL1, or full-length variants of CHL1 with the single amino acid mutation within the HPD tripeptide CHL1H1121Q (histidine exchanged to glutamine) or CHL1D1123A

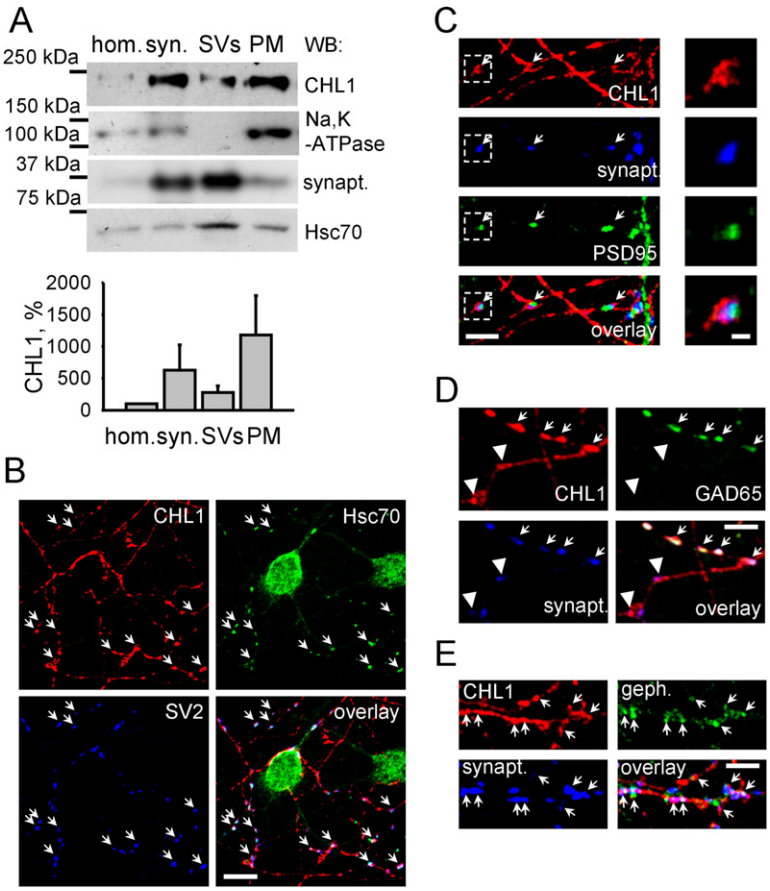

Figure 2. CHL1 Accumulates at the Presynaptic Membrane

(A) Brain homogenates (hom.), synaptosomes (syn.), crude SVs (SVs), and synaptic plasma membranes (PM) were probed by WB with antibodies against CHL1, Na,K-ATPase as a marker of plasma membranes, synaptophysin as a marker of SVs, and Hsc70. The diagram shows quantitation of CHL1 labeling from six experiments, with the optical density in the western blot of the homogenate set to 100%. Mean values ± SEM are shown. CHL1 is enriched in the synaptic plasma membrane and is present in SVs. (B–D) Hippocampal neurons were immunolabeled for cell surface, exposed CHL1 and colabeled for Hsc70 and SV2 (B), synaptophysin and PSD95 (C), GAD65 (D), or gephyrin (E). CHL1 accumulates at sites of SV2 positive synaptic boutons containing Hsc70 (B, arrows). CHL1-positive synaptic boutons marked by synaptophysin are apposed to clusters of PSD95 (C, arrows) and gephyrin (E, arrows). CHL1-positive synaptic boutons are either positive (D, arrows) or negative (D, arrowheads) for GAD65. In (C), a higher magnification of the region marked with the dashed square is shown on the right. Bars = 10 μm (B), 5 μm (C–E), 1 μm (C, higher magnification).

(aspartic acid exchanged to alanine), were transfected into Chinese hamster ovary (CHO) cells and assayed by coimmunoprecipitation for their ability to associate with endogenously expressed Hsc70. Whereas Hsc70 coimmunoprecipitated with wild-type CHL1, it did not coimmunoprecipitate with any CHL1 variant mutated in the HPD tripeptide (Figure 1D), indicating that the HPD tripeptide is essential for the binding of Hsc70 to CHL1. Furthermore, when brain lysates were incubated with an HPD tripeptide-containing 20-mer peptide derived from the CHL1-ID sequence (HPDpeptide$_{CHL1}$) and subsequently subjected to immunoprecipitation with CHL1 antibodies, Hsc70 did not coimmunoprecipitate (Figure 1E), indicating that the HPD tripeptide-containing peptide competed with endogenous CHL1 for binding to Hsc70. By contrast, preincubation with a similar peptide in which the histidine was exchanged to glutamine within the HPD tripeptide (QPDpeptide$_{CHL1}$) did not affect the complex formation between CHL1 and Hsc70. Thus, the HPD tripeptide is essential for CHL1/Hsc70 complex formation in brain tissue.

CHL1 Is Accumulated in the Presynaptic Plasma Membrane

To investigate the possibility that CHL1 is involved in the regulation of synapse functions, we analyzed the subcellular distribution of CHL1 (Figure 2A). CHL1 was enriched in synaptosomes; the level of CHL1 was approximately six times higher in synaptosomes when compared with brain homogenates. At the subsynaptic level, CHL1 was particularly enriched in the synaptic plasma membrane. Unexpectedly, we also detected CHL1 in the crude SV fraction. In both the synaptic plasma membrane and SV fractions, CHL1 cofractionated with Hsc70.

In cultured hippocampal neurons labeled with antibodies against CHL1 without permeabilization of the plasma membrane with detergent, CHL1 immunolabeling was localized to thin neurites negative for the dendritic marker MAP2 and positive for the axonal marker L1 (see Figure S1A in the Supplemental Data), indicating that CHL1 is enriched in the axonal plasma membrane. After permeabilization of neurons with detergent, intracellular CHL1 was also detected in the somata of neurons and, to a lesser extent, in their dendrites (Figure S1B). In accordance with the biochemical data, plasma membrane-associated CHL1 was highly expressed in presynaptic terminals visualized with antibodies against the SV protein SV2. In presynaptic terminals, CHL1 colocalized with Hsc70 (Figure 2B). CHL1 was detectable in both excitatory and inhibitory synapses, as indicated by apposition of CHL1 accumulations to the clusters of postsynaptic proteins of excitatory and inhibitory synapses (PSD95 and gephyrin, respectively), and by accumulation of CHL1 in synaptic boutons either positive or negative for GAD65, a presynaptic marker of inhibitory synapses (Figures 2C–2E).

CHL1 Recruits Hsc70 to Synapses

Cell adhesion molecules accumulated in synapses have been shown to anchor associated proteins at these sites (Sytnyk et al., 2004; Gerrow and El-Husseini, 2006). To analyze levels of Hsc70 in presynaptic boutons, we

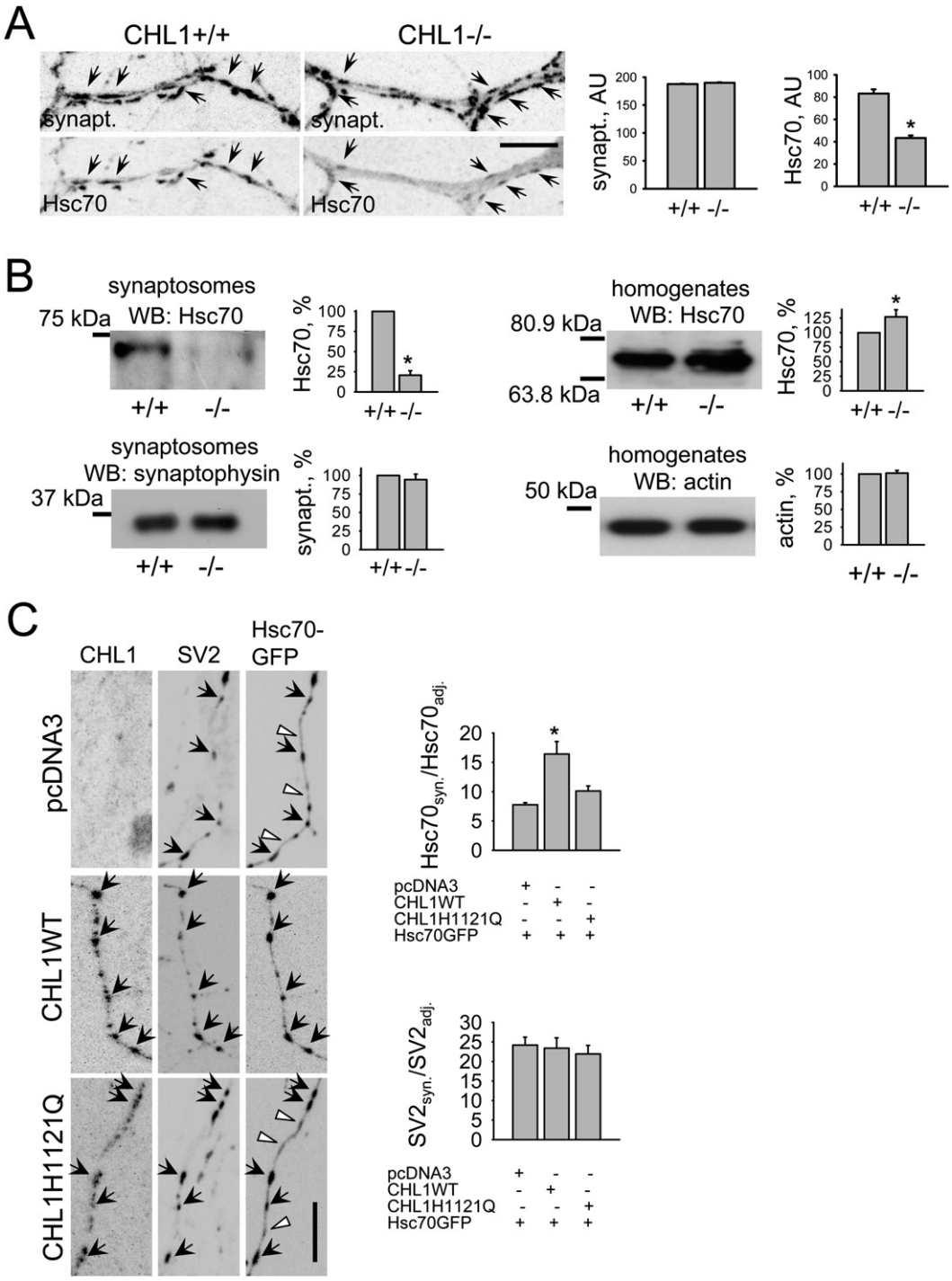

Figure 3. CHL1 Recruits Hsc70 to Synapses

(A) Neurons from *CHL1*$^{+/+}$ and *CHL1*$^{-/-}$ mice were colabeled with antibodies against synaptophysin (synapt.) and Hsc70. Immunofluorescence signals were inverted to accentuate differences in immunolabeling intensities between genotypes. Diagrams show mean intensity ± SEM of Hsc70 and synaptophysin labeling in synaptophysin clusters. AU, arbitrary units. Levels of Hsc70 are reduced in *CHL1*$^{-/-}$ versus *CHL1*$^{+/+}$ synaptic boutons (arrows). Bar = 10 μm. n > 200 synapses from images of 20 neurites from two coverslips analyzed in each group. *p < 0.05, t test.

(B) Synaptosomes and brain homogenates from *CHL1*$^{+/+}$ and *CHL1*$^{-/-}$ mice were probed by WB with antibodies against Hsc70 and synaptophysin or actin. Diagrams show quantitation of the blots from six experiments. Optical density in wild-type was set to 100%. Mean values ± SEM are shown. *p < 0.05, paired t test. Levels of Hsc70 are reduced, whereas levels of synaptophysin are not changed in *CHL1*$^{-/-}$ versus *CHL1*$^{+/+}$ synaptosomes. Levels of Hsc70 are increased, whereas levels of actin are not changed, in *CHL1*$^{-/-}$ brain homogenates.

(C) *CHL1*$^{-/-}$ neurons cotransfected with Hsc70GFP and the empty vector (pcDNA3) or vector containing full-length, wild-type CHL1 (CHL1WT) or CHL1H1121Q were colabeled with antibodies against SV2 and surface CHL1. Hsc70GFP, CHL1WT, and CHL1H1121Q accumulate in SV2 positive synaptic boutons (arrows). Inverted immunofluorescence signals are shown. Note increased extrasynaptic levels of Hsc70GFP in *CHL1*$^{-/-}$ neurons cotransfected with pcDNA3 or CHL1H1121Q (arrowheads). Bar = 10 μm. Diagrams show mean values ± SEM of the ratio of Hsc70GFP

labeled permeabilized cultured hippocampal neurons with Hsc70 antibody. Neurons were colabeled with synaptophysin antibody to identify presynaptic boutons, which were then graphically outlined to determine Hsc70 levels within the synaptophysin accumulations. Indeed, Hsc70 levels in synaptophysin accumulations were reduced in neurons derived from CHL1-deficient (*CHL1*$^{-/-}$) mice (Figure 3A). Hsc70 levels were also reduced in synaptosomes isolated from *CHL1*$^{-/-}$ brains (Figure 3B), indicating that CHL1 is involved in targeting of Hsc70 to synapses. Interestingly, Hsc70 mRNA and protein levels were slightly increased in *CHL1*$^{-/-}$ brain homogenates (Figure 3B and Figure S3), probably reflecting a compensatory reaction to inefficient targeting of the protein to synapses. This observation excludes the possibility that reduced levels of Hsc70 in synaptosomes reflect an overall decreased expression of Hsc70 in *CHL1*$^{-/-}$ brains. Levels of the SV protein synaptophysin were the same in presynaptic boutons of cultured neurons and synaptosomes from both wild-type (*CHL1*$^{+/+}$) and *CHL1*$^{-/-}$ mice (Figures 3A and 3B), showing that overall targeting of SVs was not affected in *CHL1*$^{-/-}$ brains.

To analyze the effect of CHL1 on the subcellular localization of Hsc70 in detail, we cotransfected cultured *CHL1*$^{-/-}$ neurons with wild-type CHL1 or the tripeptide mutation CHL1H1121Q together with Hsc70 tagged with green fluorescent protein (Hsc70GFP). Transfected full-length CHL1 showed a distribution similar to endogenous CHL1 expressed by *CHL1*$^{+/+}$ neurons; it was enriched in axons and SV2 antibody-labeled synaptic boutons (Figure 3C). In *CHL1*$^{-/-}$ neurons cotransfected with Hsc70GFP and the empty pcDNA3 vector, Hsc70GFP was still targeted to SV2 positive synaptic boutons. This finding indicates that cues other than CHL1 can recruit Hsc70 to synapses. Interestingly, levels of CSP, an SV-associated protein that directly binds to Hsc70, were 2-fold higher in *CHL1*$^{-/-}$ brain homogenates and synaptosomes (Figure S2), correlating with increased mRNA levels of CSP in *CHL1*$^{-/-}$ brains (Figure S3). Thus, Hsc70 may be recruited to *CHL1*$^{-/-}$ synapses by CSP. However, cotransfection with wild-type full-length CHL1 significantly enhanced the precision and degree of Hsc70GFP accumulation in synapses as determined by the ratio of Hsc70GFP levels in the center of SV2 clusters to the Hsc70 levels in the axon 3 μm away from the cluster center ($Hsc70_{syn.}/Hsc70_{adj.}$). This ratio was two times higher in CHL1 cotransfected neurons (Figure 3C). In contrast to transfection with CHL1, transfection with the CHL1H1121Q mutant did not enhance targeting of Hsc70GFP to SV2 positive synaptic boutons, showing that the interaction between the HPD tripeptide of CHL1 and Hsc70 plays a crucial role in CHL1-mediated recruitment of Hsc70 to synapses.

CHL1 Regulates Recruitment of Hsc70 to Synaptic Plasma Membranes and SVs

Interestingly, Hsc70 and CHL1 were present in both the synaptic plasma membrane and the SV fractions (Figure 2A), raising the possibility that CHL1 recruits Hsc70 to these subsynaptic compartments. Since interactions of Hsc70 with its binding partners are often regulated by nucleotides, changes in ATP/ADP concentration may provide an additional level of regulation. Thus, we tested whether ATP or ADP influence CHL1/Hsc70 complex formation. Amounts of Hsc70 that coimmunoprecipitated with CHL1 from brain lysates were approximately 4-fold higher in the presence of ADP than in the absence of nucleotides (Figure 4A), indicating that complex formation is enhanced by ADP. Interestingly, ATP reduced the efficiency of CHL1/Hsc70 complex formation to the level below the level observed in the absence of nucleotides.

To analyze the role of CHL1 and nucleotides in the recruitment of Hsc70 to the plasma membrane, synaptic plasma membrane fractions were isolated from synaptosomes of *CHL1*$^{+/+}$ and *CHL1*$^{-/-}$ brains. These fractions were then assayed for their ability to recruit Hsc70 from the soluble fraction of *CHL1*$^{+/+}$ brain homogenates used as a source of endogenous Hsc70 (Figure 4B). Before incubation with the soluble fraction, peripheral proteins in the isolated synaptic membranes were stripped by alkaline treatment to remove Hsc70 that may have been copurified. Incubation with the soluble fraction resulted in the binding of Hsc70 to *CHL1*$^{+/+}$, but not to *CHL1*$^{-/-}$, synaptic plasma membranes, indicating that CHL1 is required to recruit Hsc70 to synaptic plasma membranes. Efficiency of the binding was approximately three times higher in the presence of ADP when compared with the binding process without nucleotides, whereas addition of ATP abolished the binding.

To analyze the role of CHL1 in SVs, SVs were purified by fractionation of the crude SV fractions from *CHL1*$^{+/+}$ and *CHL1*$^{-/-}$ brains through a linear sucrose gradient followed by SV immunoisolation with the synaptophysin antibodies (Figure 4C). Purified SVs were strongly enriched in synaptophysin and were negative for the marker of the plasma membrane Na,K-ATPase and the early endosome associated protein EEA1 (not shown). Purified SVs from *CHL1*$^{+/+}$ brains contained CHL1, as revealed by immunoblot analysis (Figure 4C). Levels of Hsc70 were significantly decreased in *CHL1*$^{-/-}$ SVs compared with *CHL1*$^{+/+}$ SVs (Figure 4C), indicating that CHL1 recruits Hsc70 to SVs.

CHL1 Is Endocytosed to Synapses in Response to Synapse Activation

As a next step we tried to investigate the mechanisms that target CHL1 to SVs. As a transmembrane protein, CHL1 can be delivered to synapses in *trans*-Golgi network-derived organelles, which are then transformed to SVs (Hannah et al., 1999; Sytnyk et al., 2002; Zhai et al., 2001; Ahmari et al., 2000). However, considering the high levels of CHL1 in the synaptic plasma membrane (Figure 2A), a more potent pathway for CHL1 accumulation in SVs could be its endocytosis during SV recycling. To test the latter possibility, we analyzed the sites of CHL1 endocytosis and recycling in cultured

levels in the center of the SV2 cluster to Hsc70 levels in the adjacent axon 3 μm away from the SV2 cluster center. Cotransfection with CHL1WT enhances recruitment of Hsc70GFP to SV2 clusters, resulting in higher $Hsc70_{syn.}/Hsc70_{adj.}$ values. n > 100 synapses from ten neurons from two to three coverslips analyzed in each group. Asterisk shows a statistically significant difference when compared with pcDNA3 cotransfected neurons ($p < 0.05$, t test).

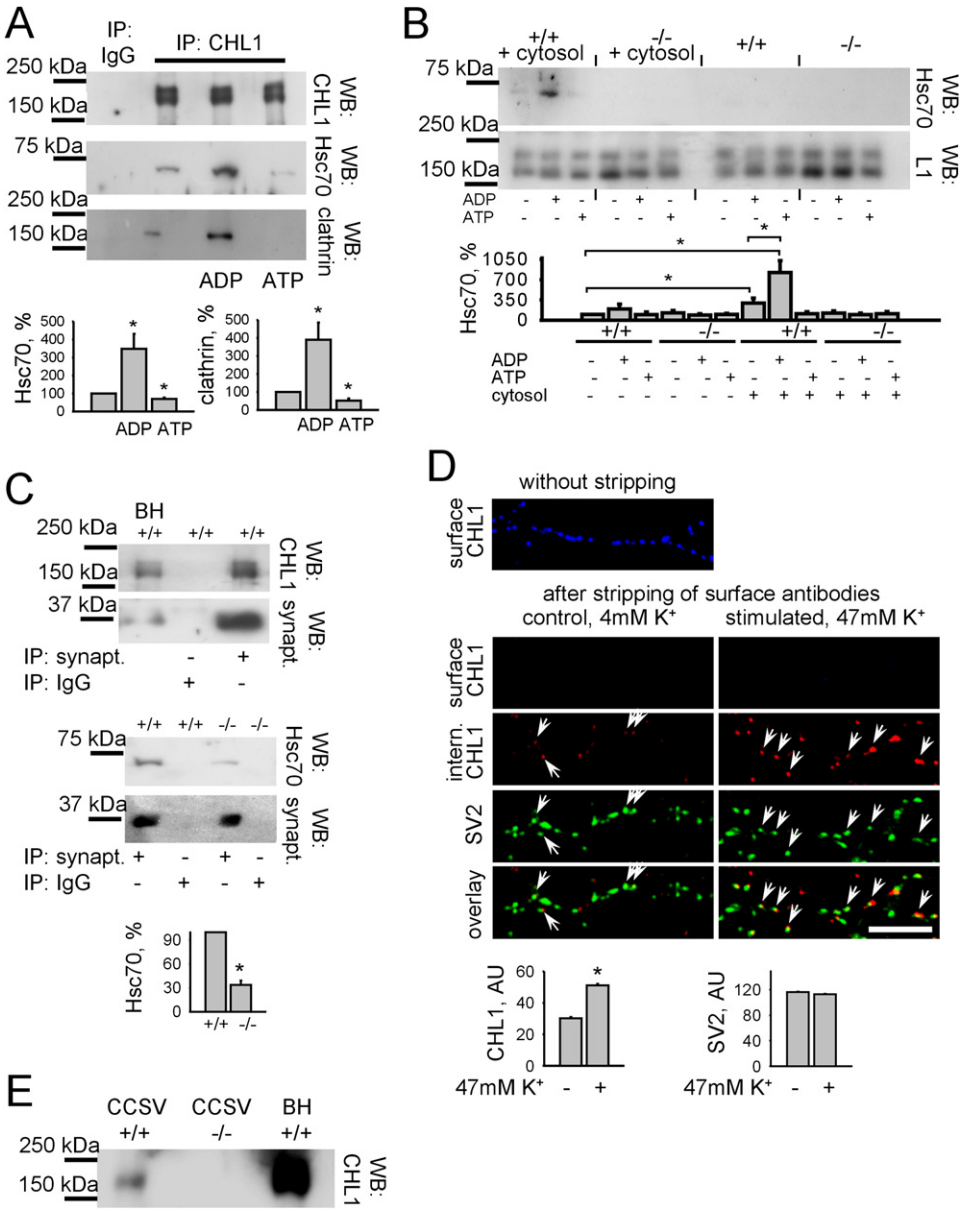

Figure 4. CHL1 Recruits Hsc70 to the Synaptic Plasma Membrane and SVs and Is Endocytosed to Synaptic Boutons in an Activity-Dependent Manner

(A) Brain lysates were preincubated with 1 mM ADP or 1 mM ATP. Similar levels of CHL1 were then IP from ADP- or ATP-treated or nontreated lysates. Immunoprecipitates were then analyzed with antibodies against Hsc70 and clathrin by WB. The diagrams show quantitation of Hsc70 and clathrin labeling with optical density for nontreated lysates set to 100%. Asterisks show statistically significant differences when compared with nontreated lysates. The highest amounts of Hsc70 and clathrin coimmunoprecipitate with CHL1 from lysates preincubated with ADP, whereas ATP reduces CHL1/Hsc70 and CHL1/clathrin coimmunoprecipitation when compared with coimmunoprecipitation in the absence of nucleotides. Immunoprecipitation with nonspecific IgG was performed for control. Diagrams show quantitation of the blots from six experiments; mean values ± SEM are shown; *$p < 0.05$, paired t test.

(B) Synaptic plasma membranes from *CHL1*$^{+/+}$ or *CHL1*$^{-/-}$ brains were preincubated with the soluble fraction of brain homogenates (cytosol) from *CHL1*$^{+/+}$ brains in the presence or absence of 1 mM ADP or 1 mM ATP. Amounts of Hsc70 derived from the soluble fraction that had bound to the membranes were then estimated by WB. Labeling with L1 antibodies shows that similar amounts of isolated synaptic plasma membranes were used in each group. The diagram shows quantitation of Hsc70 labeling with optical density for nontreated *CHL1*$^{+/+}$ synaptic membranes set to 100%. Hsc70 binds only to *CHL1*$^{+/+}$ membranes, with highest efficiency of binding in the presence of ADP. Diagrams show quantitation of the blots from six experiments; mean values ± SEM are shown; *$p < 0.05$, paired t test.

(C) *CHL1*$^{+/+}$ and *CHL1*$^{-/-}$ SVs IP with antibodies against synaptophysin (IP: synapt.) were probed by WB with antibodies against CHL1, synaptophysin, and Hsc70. Note that *CHL1*$^{+/+}$ SVs contain CHL1. Brain homogenate (BH) is shown for comparison. Diagram shows quantitation of Hsc70 levels with the optical density in *CHL1*$^{+/+}$ set to 100%. Hsc70 levels are reduced in *CHL1*$^{-/-}$ SVs. Immunoprecipitation with nonspecific IgG was performed for control. Diagrams show quantitation of the blots from six experiments; mean values ± SEM are shown; *$p < 0.05$, paired t test.

(D) Live neurons were incubated with antibodies against CHL1 and allowed to internalize the antibodies in the presence of nominal (4 mM) or high (47 mM) K^+. Immunolabeling of surface bound antibodies (surface CHL1) in neurons fixed without stripping shows that the antibodies bound to

hippocampal neurons by visualizing CHL1-mediated uptake of cell surface bound CHL1 antibodies to intracellular organelles (Carroll et al., 1999). CHL1 antibodies were applied to live cultured neurons in culture medium, and neurons were then allowed to incorporate CHL1 antibodies either at resting conditions in the presence of nominal 4 mM K^+ or in the presence of 47 mM K^+ applied to stimulate exo- and endocytosis of SVs by depolarizing neuronal plasma membranes and inducing Ca^{2+} influx (Virmani et al., 2003). Antibodies bound to CHL1 at the cell surface were then removed by exposure to 0.5 M NaCl/0.2 M acetic acid, a procedure that did not result in abnormal swelling or degeneration of cells (not shown). Following permeabilization of neurons with detergent, internalized CHL1/CHL1 antibody complexes, resistant to acid stripping, were detected with fluorescence-labeled secondary antibodies (Figure 4D; Carroll et al., 1999). Colabeling with SV2 antibodies showed that the major sites of CHL1 antibody uptake colocalized with SV2 accumulations (Figure 4D). CHL1 was endocytosed to synaptic boutons even at resting conditions, probably due to antibody induced cross-linking of CHL1 at the cell surface, followed by internalization and/or basal synaptic activity in cultures. However, stimulation with high K^+ enhanced CHL1 endocytosis to synaptic boutons: levels of CHL1 antibody internalized to SV2 positive synaptic boutons of neurons stimulated by high K^+ were approximately two times higher than those of nonstimulated neurons (Figure 4D).

To analyze the mechanisms by which CHL1 is endocytosed in synaptic boutons, we investigated whether CHL1 is present in CCSVs representing structural intermediates in the clathrin-dependent SV recycling pathway. Immunoblot analysis of the CCSVs isolated from brain tissue (Maycox et al., 1992) showed that CCSVs contained CHL1 (Figure 4E). Clathrin coimmunoprecipitated with CHL1 from brain lysates, and the CHL1/clathrin complex formation was potentiated by ADP and inhibited by ATP in a manner similar to the regulation of the CHL1/Hsc70 complex (Figure 4A). Endocytosed CHL1 immunoreactive structures often appeared aside the major synaptic vesicle cluster labeled with antibodies against SV2 (Figure 4D), as has been reported before for CCSVs (Bloom et al., 2003). The combined observations indicate that CHL1 is endocytosed via a clathrin-dependent pathway to be targeted to SVs in response to synapse activation.

CHL1 Regulates Clathrin Uncoating from CCSVs

In neurons and nonneuronal cells, Hsc70 is the major ATPase mediating clathrin uncoating from clathrin-coated vesicles (Newmyer and Schmid, 2001). In synapses, Hsc70 uncoates clathrin from SVs recycling via a clathrin-dependent pathway (Zinsmaier and Bronk, 2001; Morgan et al., 2001). We therefore investigated whether abnormalities in subcellular distribution of Hsc70 in *CHL1*$^{-/-}$ brains may affect levels of clathrin expression. Indeed, the intensity of clathrin labeling measured in synaptophysin clusters was slightly increased in cultured *CHL1*$^{-/-}$ versus *CHL1*$^{+/+}$ neurons (Figure 5A). Protein and mRNA levels of clathrin were also higher in *CHL1*$^{-/-}$ brain homogenates (Figure 5B and Figure S3) and levels of clathrin protein were increased in *CHL1*$^{-/-}$ synaptosomes and purified SVs (Figures 5B and 5C), suggesting that CHL1 is important for clathrin uncoating from SVs. To assess the role of CHL1 in clathrin release from SVs, we isolated CCSVs from *CHL1*$^{+/+}$ and *CHL1*$^{-/-}$ brains (Maycox et al., 1992) and analyzed the rate of clathrin release from CCSVs in response to application of an ATP-regenerating cocktail. The extent of CCSV uncoating was assayed by following the transfer of the clathrin heavy chain from the pellet to the supernatant after centrifuge sedimentation of the vesicles (Chang et al., 2002). ATP-regenerating cocktail induced rapid clathrin uncoating from *CHL1*$^{+/+}$ CCSVs, resulting in the release of 70%–100% of clathrin within 3–15 min (Figure 6), indicating that Hsc70, which copurifies with CHL1$^{+/+}$ SVs (Figure 2A), was sufficient for clathrin release from these vesicles in the presence of ATP. In contrast, clathrin release from *CHL1*$^{-/-}$ CCSVs was severely impaired, resulting in the release of only 10% of all clathrin after 15 min of buffer application (Figure 6). A similarly impaired clathrin release was also observed when *CHL1*$^{+/+}$ CCSVs were preincubated with recombinant CHL1-ID or $HPDpeptide_{CHL1}$, thus inducing competition between endogenous CHL1 in SVs and recombinant CHL1-ID or $HPDpeptide_{CHL1}$ for peripheral proteins associated with vesicles, including Hsc70 (Figure 6). In contrast, $QPDpeptide_{CHL1}$ did not affect clathrin uncoating, indicating that the HPD motif is essential for CHL1-regulated clathrin release. Preincubation of CCSVs with two other binding partners of Hsc70, recombinant CSP (Tobaben et al., 2001) or BAG-1 (Takayama et al., 1999), also did not affect clathrin uncoating (Figure 6), indicating specificity for CHL1. Furthermore, when 400 nM recombinant Hsc70 was included in the ATP-regenerating cocktail during the CCSV uncoating reaction, the rate and extent of clathrin release from *CHL1*$^{-/-}$ CCSVs were increased to *CHL1*$^{+/+}$ levels (Figure 6). The combined observations indicate that CHL1 regulates clathrin release from CCSVs by recruiting Hsc70 to their surface.

Activity-Induced Formation of CCSVs Is Reduced after CHL1/Hsc70 Complex Disruption

To investigate whether abnormalities in clathrin release affect formation of CCSVs in an activity-dependent manner, we analyzed numbers of CCSVs in synapses of nontreated versus high K^+-stimulated *CHL1*$^{+/+}$ and *CHL1*$^{-/-}$ neurons by means of electron microscopy. The number of CCSVs was increased in presynaptic boutons of morphologically identified synapses of nontreated *CHL1*$^{-/-}$ neurons (Figure 7A), indicating that uncoating of CCSVs

the surface. Surface bound antibodies were then stripped. The surface bound antibodies are not detectable in neurons after stripping. Accumulations of internalized CHL1 antibodies (intern. CHL1) overlap with SV2 positive synaptic boutons. Diagrams show mean intensity ± SEM of SV2 labeling and endocytosed CHL1 labeling in SV2 clusters. AU, arbitrary units. Levels of internalized CHL1, but not of endogenous SV2, in SV2 positive synaptic boutons are higher after high K^+ stimulation, indicating that SV recycling induced by high K^+ enhances CHL1 endocytosis in synapses. Bar = 10 μm. n > 1600 synapses from 20 neurons from two coverslips analyzed in each group. *p < 0.05, t test.
(E) *CHL1*$^{+/+}$ and *CHL1*$^{-/-}$ CCSVs were probed by WB with antibodies against CHL1. Note that CHL1 is present in *CHL1*$^{+/+}$ CCSVs. BH is shown for comparison.

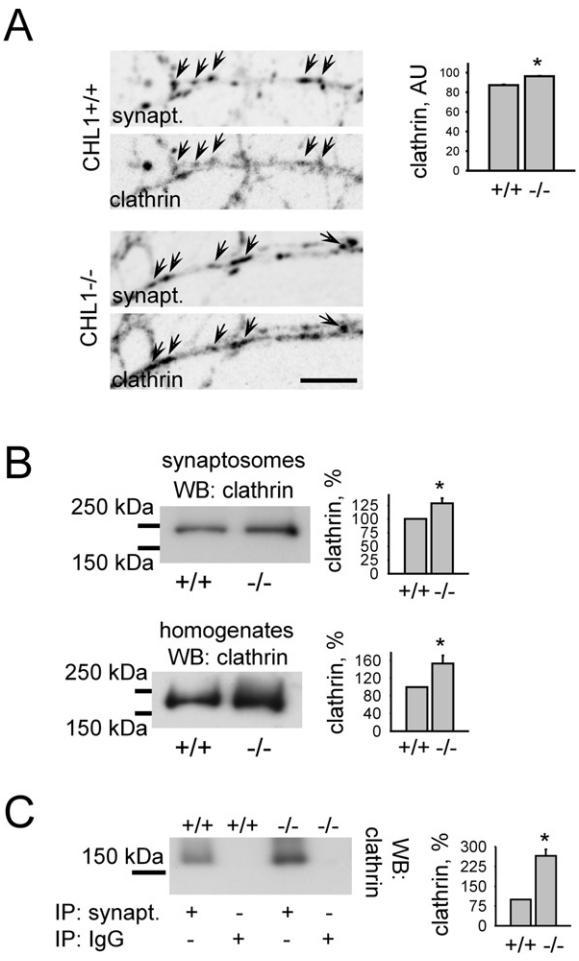

Figure 5. *CHL1*$^{-/-}$ Synapses Contain Increased Levels of Clathrin

(A) *CHL1*$^{+/+}$ and *CHL1*$^{-/-}$ neurons were colabeled with antibodies against synaptophysin and clathrin (clath.). Immunofluorescence signals were inverted to accentuate differences in immunolabeling intensities between genotypes. Diagrams show mean intensity ± SEM of clathrin labeling in synaptophysin clusters. AU, arbitrary units. Levels of clathrin are increased in *CHL1*$^{-/-}$ versus *CHL1*$^{+/+}$ synaptic boutons (arrows). Bar = 10 μm. n > 5000 synapses from 20 neurons from two coverslips analyzed in each group. *p < 0.05, t test. (B and C) *CHL1*$^{+/+}$ and *CHL1*$^{-/-}$ synaptosomes and brain homogenates (B) and SVs IP with antibodies against synaptophysin (C) were probed by WB with antibodies against clathrin. In (C), immunoprecipitation with nonspecific IgG was performed for control. Diagrams show quantitation of blots from six experiments. Optical density in *CHL1*$^{+/+}$ was set to 100%. Mean values ± SEM are shown. *p < 0.05, paired t test. Levels of clathrin are increased in *CHL1*$^{-/-}$ versus *CHL1*$^{+/+}$ synaptosomes, brain homogenates, and SVs.

formed under conditions of spontaneous activity in culture was inhibited when compared with *CHL1*$^{+/+}$ synapses. Already 10 s after application of high K^+-containing buffer (the earliest time tested), the number of CCSVs increased in *CHL1*$^{+/+}$ boutons, reached a peak at 30 s after high K^+ application, and slightly declined by 90 s at the end of stimulation by high K^+. Five minutes after exchanging the high K^+ buffer to the nominal K^+ buffer, the number of CCSVs in *CHL1*$^{+/+}$ boutons declined to the level observed in nonstimulated neurons. In contrast, the number of CCSVs in *CHL1*$^{-/-}$ boutons only slightly increased in response to high K^+ and remained at this level until the end of stimulation, suggesting that inhibition of uncoating of CCSVs in *CHL1*$^{-/-}$ boutons hampered activity-induced formation of new CCSVs. This effect was particularly evident when activity-induced changes in the numbers of CCSVs were compared: in *CHL1*$^{+/+}$ boutons, the number of CCSVs increased by a factor of 2.6 in response to high K^+, whereas in *CHL1*$^{-/-}$ neurons, this increased by only a factor of 1.6 (Figures 7A and 7C). Inhibited formation of CCSVs was not related to a defect in SV exocytosis, since a reduction in the total number of SVs in response to high K^+ (indicative of SVs that had fused with the plasma membrane) was similar in *CHL1*$^{+/+}$ and *CHL1*$^{-/-}$ synapses (Figure 7C). Similarly, exocytosis was normal in *CHL1*$^{-/-}$ synapses as measured by electrophysiological recordings (Nikonenko et al., 2006). Other parameters with impact on the efficacy of neurotransmission, such as number of mitochondria, lengths of active zones in *CHL1*$^{-/-}$ synapses, and number of perforated synapses in *CHL1*$^{-/-}$ neurons were also normal (Figure S4).

The relatively mild phenotype of *CHL1*$^{-/-}$ synapses at resting conditions could be explained by compensatory mechanisms. In particular, while mRNA and protein levels of Hsp70, an inducible counterpart of Hsc70, were slightly decreased in *CHL1*$^{-/-}$ brain homogenates (Figures S2 and S3), Hsp70 protein levels were increased by approximately 60% in *CHL1*$^{-/-}$ synaptosomes and SVs (Figure S2), suggesting that Hsp70 is recruited to *CHL1*$^{-/-}$ synapses instead of Hsc70, thus at least partially substituting for Hsc70—a phenomenon observed in an Hsc70-4 *Drosophila* mutant (Bronk et al., 2001). To analyze the consequences of an acute CHL1/Hsc70 complex disruption, we introduced $HPDpeptide_{CHL1}$ into live neurons, thus interfering with Hsc70 binding to CHL1 in a dominant-negative fashion (Figure 1E). Loading neurons with $HPDpeptide_{CHL1}$, but not with $QPDpeptide_{CHL1}$, or mock treatment of neurons with the peptide delivering reagent resulted in a 2-fold increase in the number of CCSVs at resting conditions and a profound reduction of CCSV formation in response to high K^+ (Figures 7B and 7C). Furthermore, in neurons loaded with $HPDpeptide_{CHL1}$, the total number of SVs was reduced at resting conditions. The total number of SVs in $HPDpeptide_{CHL1}$-loaded synapses decreased in response to high K^+, indicating that SV exocytosis was not blocked. However, the amplitude of this decrease was smaller in $HPDpeptide_{CHL1}$-loaded synapses when compared with mock- or $QPDpeptide_{CHL1}$- treated neurons. Western blot analysis of lysates of the peptide-treated cultures showed that the total levels of CSP and Hsp70 were not changed in $HPDpeptide_{CHL1}$-loaded neurons (Figure S5A), indicating that compensatory mechanisms were not active at the time the cultures were analyzed. The levels of Hsp70 and CSP were slightly decreased in synaptophysin accumulations in neurons treated with $HPDpeptide_{CHL1}$ (Figure S5B)—an effect that was probably related to a reduced number of SVs in these synapses.

Changes in the numbers of CCSVs correlated with the changes in the levels of Hsc70 and clathrin in synaptophysin accumulations in neurons treated with high K^+ (Figure 7D). In mock- or $QPDpeptide_{CHL1}$-loaded neurons, synaptic levels of Hsc70 and clathrin increased 30 s after application of high K^+ and returned to initial levels 5 min after a 90 s stimulation with high K^+. In nonstimulated neurons loaded with $HPDpeptide_{CHL1}$, levels

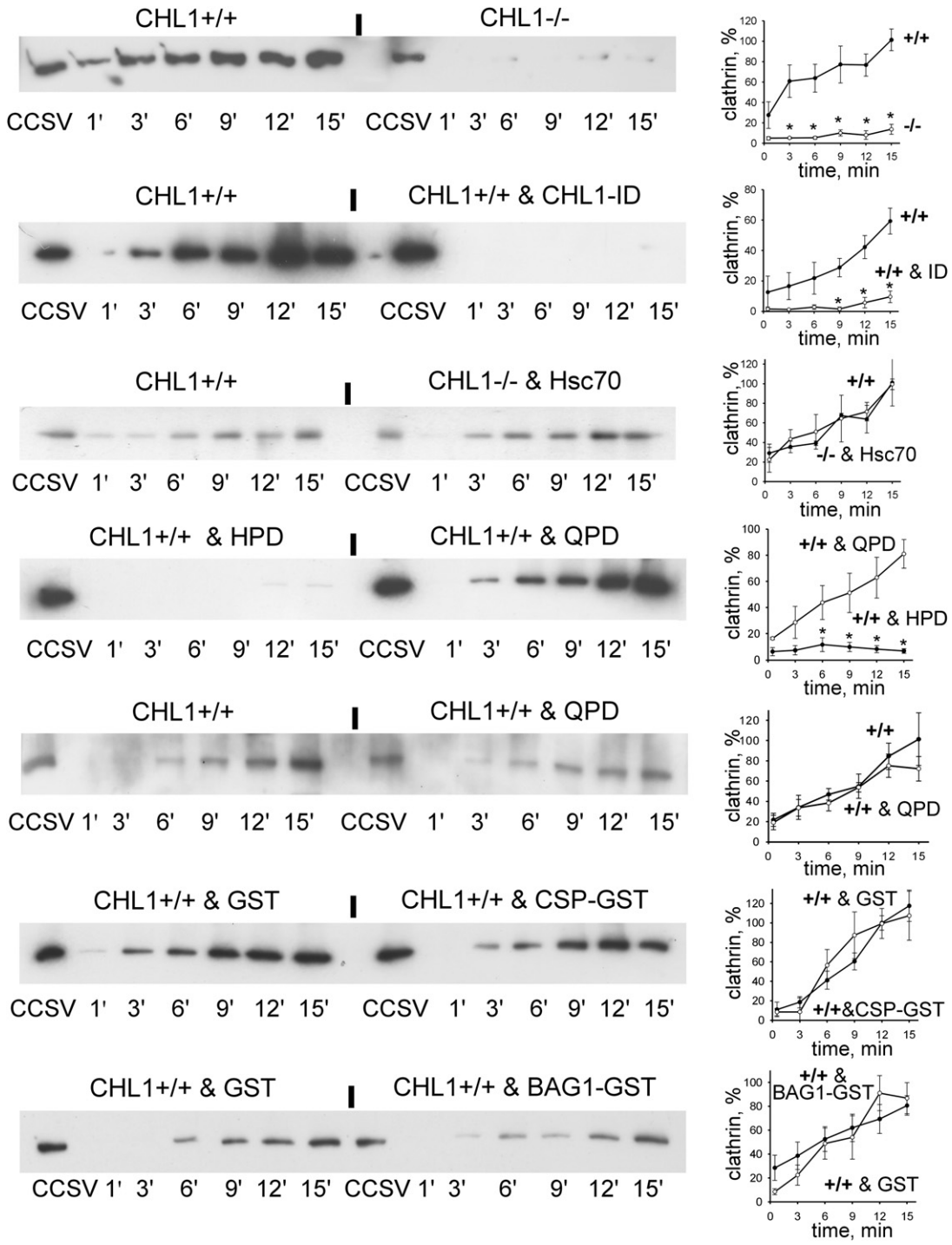

Figure 6. CHL1 Regulates Uncoating of Clathrin from Synaptic Vesicles

Isolated CCSVs were used for the in vitro clathrin uncoating assay. CCSVs before initiation of the uncoating reaction and clathrin released from CCSVs after initiation of clathrin uncoating, collected at indicated time points (in minutes), were probed by WB with antibodies against clathrin. Experiments were performed for $CHL1^{+/+}$ and $CHL1^{-/-}$ CCSVs in the absence or presence of recombinant proteins or $HPDpeptide_{CHL1}$ (HPD) or $QPDpeptide_{CHL1}$ (QPD) peptides as indicated. Diagrams show quantitation of the blots from six experiments with optical density for untreated CCSVs set to 100%. Mean values ± SEM are shown. *$p < 0.05$, paired t test. Note the strongly reduced uncoating of clathrin from $CHL1^{-/-}$ CCSVs and $CHL1^{+/+}$ CCSVs preincubated with 167 nM CHL1-ID or 400 nM $HPDpeptide_{CHL1}$. Efficiency of $CHL1^{-/-}$ CCSV uncoating is increased to $CHL1^{+/+}$ levels by application of 400 nM recombinant Hsc70 during the uncoating reaction. Uncoating of clathrin is not affected by 400 nM $QPDpeptide_{CHL1}$, 400 nM CSP, or 400 nM BAG-1.

of clathrin were increased, whereas levels of Hsc70 were decreased in synaptophysin clusters. The increase in synaptic levels of clathrin and Hsc70 in response to high K^+ in these neurons was attenuated. These observations indicate that CHL1 recruits Hsc70 to synaptic boutons not only at resting conditions, but even more

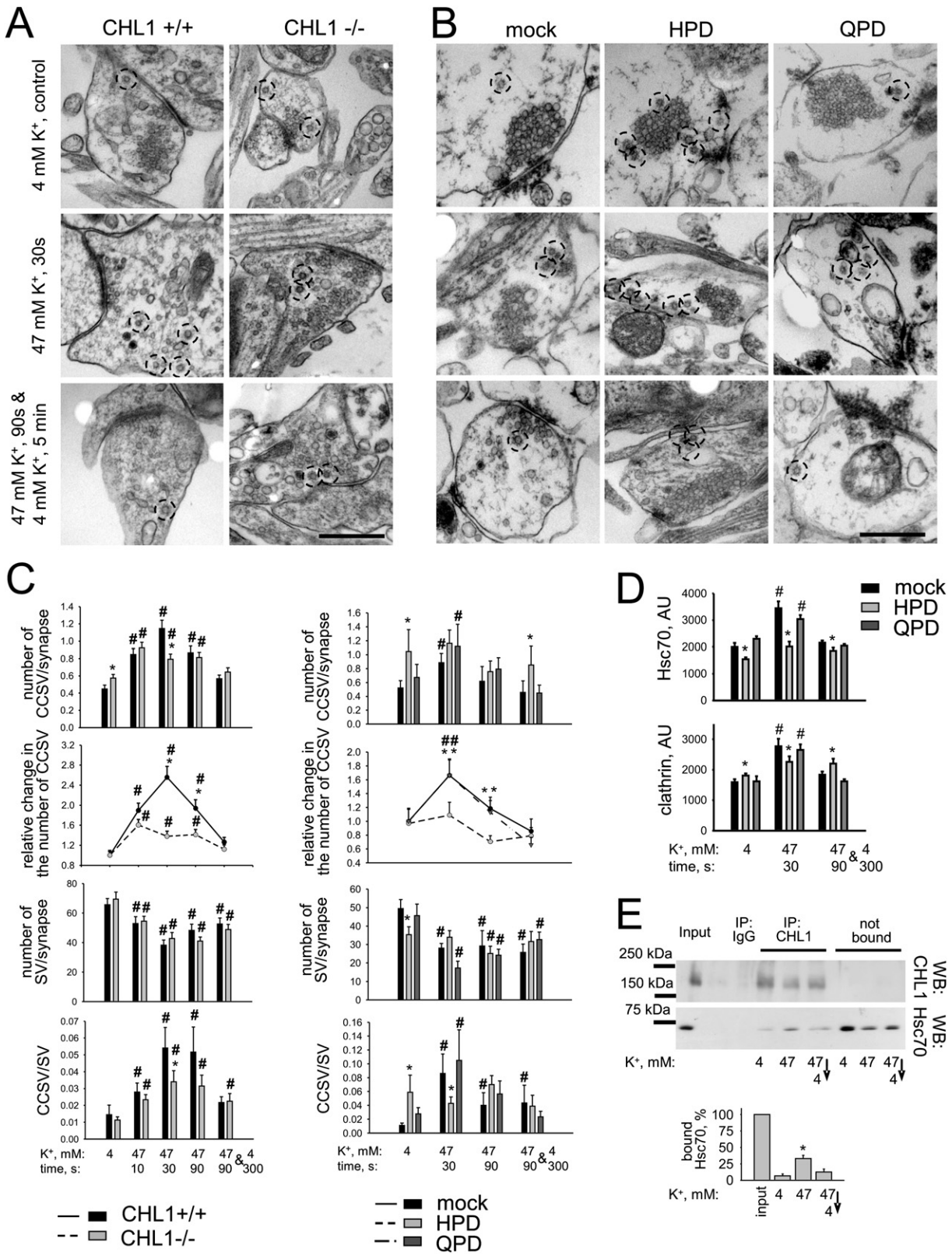

Figure 7. Activity-Induced Formation of Clathrin-Coated Synaptic Vesicles Is Inhibited in *CHL1*$^{-/-}$ Synapses and in *CHL1*$^{+/+}$ Synapses in which the CHL1/Hsc70 Complex Is Disrupted

(A–D) *CHL1*$^{+/+}$ and *CHL1*$^{-/-}$ neurons (A and C) or *CHL1*$^{+/+}$ neurons loaded with HPDpeptide$_{CHL1}$ (HPD) or QPDpeptide$_{CHL1}$ (QPD), or mock-treated with the peptide delivering reagent (B–D), were incubated in modified Tyrode solution containing 4 mM K^+ (control) or 47 mM K^+ for the indicated time intervals or allowed to recover for 5 min at 4 mM K^+ before fixation. Neurons were fixed for electron microscopy (A–C) or immunofluorescence analysis (D). (A and B) Representative electron micrographs for conditions indicated in (A) (for A and B) are shown. CCSVs are

efficiently after activation, allowing for dynamic changes in clathrin levels at the synapse in response to synaptic activity. To understand the nature of CHL1-mediated recruitment of Hsc70 to activated synapses, we immunoprecipitated CHL1 from nonstimulated or stimulated synaptosomes. Approximately 6% and 33% of all Hsc70 coimmunoprecipitated with CHL1 from nonstimulated and stimulated synaptosomes, respectively, suggesting a potentiated interaction between CHL1 and Hsc70 in activated synapses (Figure 7E). This effect was reversible; levels of coimmunoprecipitated Hsc70 decreased to 13% after withdrawal of high K^+.

Activity-Dependent Uptake and Release of FM Dyes Are Reduced in Synaptic Boutons after CHL1/Hsc70 Complex Disruption

To corroborate our finding that abnormalities in clathrin uncoating in *CHL1*$^{-/-}$ synaptic boutons affect recycling of SVs, we analyzed the efficiency of FM dye uptake to synaptic boutons of cultured *CHL1*$^{+/+}$ or *CHL1*$^{-/-}$ neurons in response to stimulation with high K^+. Uptake of FM4-64 applied in high K^+-containing buffer for 90 s, a protocol that labels the total pool of SVs recycling via clathrin-dependent and -independent pathways (Virmani et al., 2003), was only slightly decreased in *CHL1*$^{-/-}$ synaptic boutons when compared with *CHL1*$^{+/+}$ synaptic boutons (Figure 8A). In contrast to the uptake of the highly lipophilic FM4-64 dye, uptake of the less lipophilic FM2-10 dye is more sensitive to the rate of endocytosis, since this dye can be washed away more readily from the relatively slowly forming invaginations of synaptic plasma membranes preceding endocytosis via the clathrin-dependent pathway (Richards et al., 2000; Virmani et al., 2003). The amount of FM2-10 taken up into *CHL1*$^{-/-}$ synaptic boutons was reduced by approximately 50% when compared with *CHL1*$^{+/+}$ neurons (Figure 8A). We also used a fixable analog of FM1-43—FM1-43FX, allowing us to analyze dye uptake in relation to the size of SV clusters visualized with SV2 antibodies after fixation of the neurons. Whereas SV2 accumulations did not differ in *CHL1*$^{+/+}$ and *CHL1*$^{-/-}$ neurons, levels of FM1-43FX, which is less lipophilic than FM4-64 but more lipophilic than FM2-10, were also reduced when measured in SV2 clusters in *CHL1*$^{-/-}$ neurons. The changes in FM1-43FX uptake were smaller than changes observed for FM2-10 but larger than those for FM4-64 (Figure 8B). A similarly reduced FM1-43FX uptake was observed in *CHL1*$^{+/+}$ neurons loaded with HPDpeptide$_{CHL1}$ (Figure 8C). SV2 accumulations in these neurons were also reduced, in agreement with our observation that the number of SVs in synapses is reduced after introduction of HPDpeptide$_{CHL1}$.

A reduced processing of SVs via clathrin-dependent recycling could make them unavailable for exocytosis in response to the next stimulus. Interestingly, in accordance with this idea, when synaptic boutons in *CHL1*$^{+/+}$ and *CHL1*$^{-/-}$ cultures were loaded with FM4-64 at high K^+, and when release of the dye from synaptic boutons identified by FM4-64 labeling was induced by a second pulse of high K^+, the rate of FM4-64 release was significantly reduced in *CHL1*$^{-/-}$ synaptic boutons (Figure 8D). A similar effect was observed in *CHL1*$^{+/+}$ neurons after introduction of HPDpeptide$_{CHL1}$ (Figure 8E). In summary, these observations suggest that reduced clathrin uncoating from SVs slows the rate of SV recycling either in *CHL1*$^{-/-}$ synapses or after disruption of the CHL1/Hsc70 complex by an interfering peptide.

Discussion

We demonstrate a role for the cell adhesion molecule CHL1 in the regulation of uncoating of CCSVs: to control uncoating of CCSVs, CHL1 associates with the constitutively expressed heat shock cognate Hsc70. Interestingly, we found that high levels of Hsc70 cofractionate with CHL1 in the synaptic membrane fraction, indicating that Hsc70 forms a complex with CHL1 in the plasma membrane. CHL1-mediated recruitment of Hsc70 is significantly enhanced in the presence of ADP, whereas CHL1/Hsc70 complex is dissociated by ATP. ATP-depleting, and thus ADP-producing, reactions accompany fusion of SVs (Sollner et al., 1993) and/or initiation of clathrin coat assembly (Schmid and Smythe, 1991) and should result in a local increase in ADP concentration beneath the plasma membrane. It is thus tempting to speculate that this increase in ADP concentration promotes activity-dependent CHL1/Hsc70 complex formation as observed in isolated synaptosomes, thereby inducing an initial CHL1-dependent recruitment of Hsc70 to the synaptic plasma membrane. Interestingly, the Hsc70 binding partner auxilin is also initially recruited to the growing clathrin cages and budding vesicles at the cell surface (Massol et al., 2006). Following ATP-independent invagination of clathrin-coated pits (Mahaffey et al., 1989; Smythe et al., 1989) and ATP/GTP-dependent budding of the vesicles (Carter et al., 1993; Schmid and Smythe, 1991), CCSVs translocate to the synapse interior away from the ATP-depleted area

marked with dashed circles. Bars = 0.5 μm. (C) Diagrams show numbers of CCSVs per synaptic bouton profile, changes in the number of CCSVs with respect to control neurons, total number of SVs, and the ratio of CCSV number to total SV number. Mean numbers ± SEM are shown. Note increased numbers of CCSVs in control and reduced increase in numbers of CCSVs in response to high K^+ in *CHL1*$^{-/-}$ neurons and HPDpeptide$_{CHL1}$-loaded *CHL1*$^{+/+}$ neurons. n > 200 synapses from at least four coverslips analyzed in each group. *p < 0.05, t test. (D) Neurons were colabeled with antibodies against synaptophysin, Hsc70, and clathrin. Levels of Hsc70 and clathrin were measured in synaptophysin accumulations. Note slightly increased levels of clathrin and reduced levels of Hsc70 in HPDpeptide$_{CHL1}$-loaded neurons at resting conditions, and reduced increase of synaptic Hsc70 and clathrin levels in these neurons in response to high K^+. n > 5000 synapses from 30 neurons from three coverslips analyzed in each group. In (C) and (D), *p < 0.05, t test indicates differences between *CHL1*$^{-/-}$ and *CHL1*$^{+/+}$ neurons or between HPDpeptide$_{CHL1}$- and mock-loaded neurons. #p < 0.05, t test shows statistically significant difference when neurons of the same genotype or neurons loaded with the same peptide are compared with the control group of neurons of a particular genotype or the control group loaded with a particular peptide. (E) CHL1 was IP from nontreated or high K^+-treated synaptosomes. In the third group, high K^+ was applied for 90 s and immediately exchanged with the nominal K^+. Immunoprecipitates, protein input, and material not bound to the beads were probed by WB with antibodies against CHL1 and Hsc70. Diagram shows quantitation of coimmunoprecipitated Hsc70 levels from four experiments with optical density for the input material set to 100%. Mean values ± SEM are shown. *p < 0.05, paired t test. Level of coimmunoprecipitated Hsc70 is increased in response to high K^+.

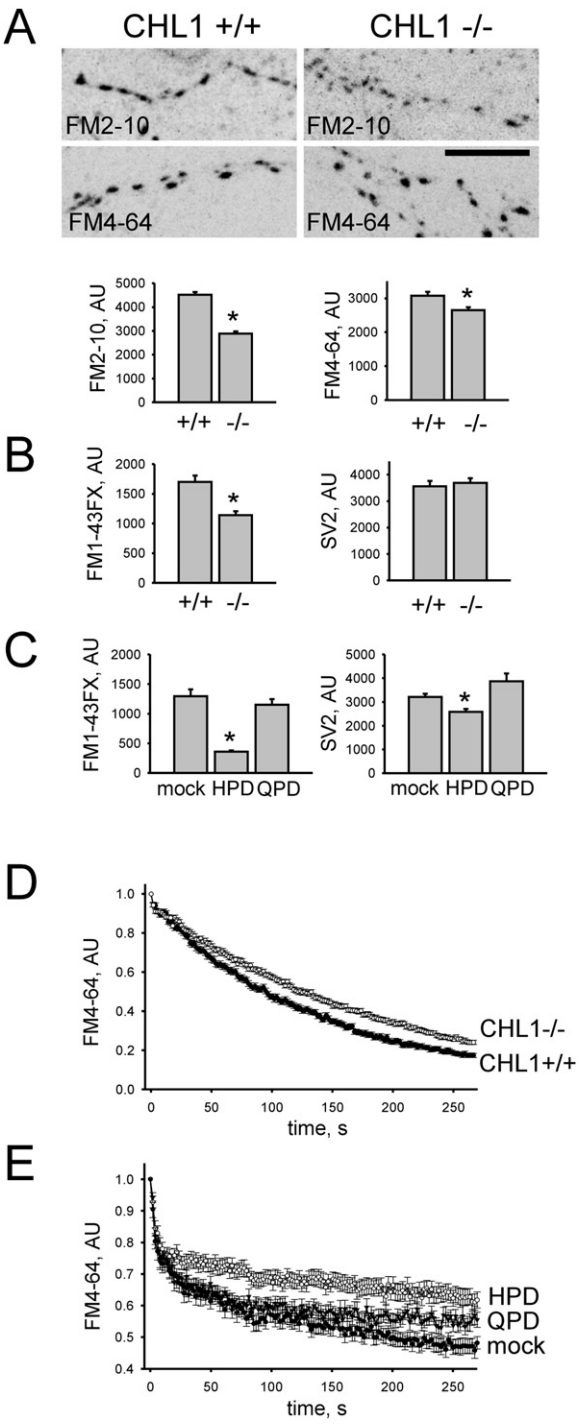

Figure 8. Synaptic Vesicle Recycling Is Inhibited in *CHL1*$^{-/-}$ Synapses and *CHL1*$^{+/+}$ Synapses in which the CHL1/Hsc70 Complex Is Disrupted

(A) *CHL1*$^{+/+}$ and *CHL1*$^{-/-}$ neurons were incubated in high K^+ for 90 s in the presence of FM4-64 or FM2-10 dyes. Diagrams show mean values ± SEM of FM dye intensity in FM dye cluster multiplied by the cluster area. AU, arbitrary units. Note reduced uptake of FM2-10 and slightly reduced uptake of FM4-64 into *CHL1*$^{-/-}$ synapses. n > 600 synapses from 20 neurons from four coverslips analyzed in each group. *p < 0.05, t test. Bar = 10 μm.

(B and C) *CHL1*$^{+/+}$ and *CHL1*$^{-/-}$ neurons (B) or *CHL1*$^{+/+}$ neurons loaded with $HPDpeptide_{CHL1}$ (HPD) or $QPDpeptide_{CHL1}$ (QPD), or mock-treated (C), were incubated in high K^+ for 90 s in the presence of FM1-43FX, fixed, and colabeled with SV2 antibodies. Diagrams show mean values ± SEM of FM1-43FX or SV2 intensity in SV2 clusters multiplied by the cluster area. AU, arbitrary units. Note reduced uptake of FM1-43FX to synaptic boutons in *CHL1*$^{-/-}$ or *CHL1*$^{+/+}$ neurons loaded with $HPDpeptide_{CHL1}$. n > 2000 synapses from 30 neurons from three coverslips analyzed in each group. *p < 0.05, t test.

(D and E) Synapses of *CHL1*$^{+/+}$ and *CHL1*$^{-/-}$ neurons (D) or *CHL1*$^{+/+}$ neurons loaded with $HPDpeptide_{CHL1}$ (HPD) or $QPDpeptide_{CHL1}$ (QPD), or mock-treated (E), were loaded with FM4-64 by incubation in high K^+ for 90 s in the presence of the dye. After washing in modified Tyrode solution containing normal levels of K^+, high K^+ was again applied and FM4-64 release from the synapses was monitored with time. The diagram shows mean values ± SEM of FM4-64 intensity in FM4-64 clusters at the indicated time points after high K^+ application. For each synaptic bouton, FM4-64 intensity values immediately before application of high K^+ were set to 1. Note reduced rate of FM4-64 release from synaptic boutons of *CHL1*$^{-/-}$ and $HPDpeptide_{CHL1}$-loaded *CHL1*$^{+/+}$ neurons. Forty seconds after initiation of the FM4-64 release, the difference became statistically significant and remained statistically significant for each time point until the end of the recordings (p < 0.05, t test, not depicted in the figure). n > 100 synapses from five neurons from five coverslips analyzed in each group.

beneath the plasma membrane. This should result in an increase in ATP concentration that would dissociate the CHL1/Hsc70 complex and promote binding of Hsc70 to auxilin, accompanied by ATP-dependent clathrin release.

This scenario suggests that CHL1 is endocytosed to SVs. Indeed, we found that CHL1 is present in a highly purified fraction of SVs and is endocytosed to synapses in response to synapse activation. The recycling pool of SVs in hippocampal synapses comprises only 10%–20% of SVs, with an even smaller fraction of SVs recycling via the clathrin-dependent pathway (Rizzoli and Betz, 2005; Harata et al., 2001). Thus, only a subpopulation of SVs should contain CHL1, which is targeted to recycling SVs from the axonal plasma membrane by endocytosis. The intracellular domain of CHL1 contains binding motifs for the adaptor protein AP2 that could recruit CHL1 to the budding CCSVs. This adaptor protein, which is enriched in the presynaptic membrane (Yao et al., 2002), coordinates clathrin coat assembly and recruitment of the cargo proteins to the budding clathrin-coated vesicles (Schmid, 1997). Accordingly, we show that CHL1 is present in CCSVs and associates with clathrin. Interestingly, ADP promotes not only CHL1/Hsc70, but also CHL1/clathrin, complex formation, indicating that ATP-consuming, and thus ADP-producing, fusion of SVs may promote redistribution of the CHL1/Hsc70 complex to clathrin-coated pits and budding vesicles. The CHL1/clathrin complex dissociates in the presence of ATP, indicating that an increase in ATP concentration in the vicinity of the CHL1-containing CCSVs should induce not only dissociation of Hsc70, but also of clathrin, from CHL1, thus further promoting clathrin release from the vesicle.

Levels of Hsc70 associated with SVs are strongly reduced in *CHL1*$^{-/-}$ mice, indicating that CHL1 not only recruits Hsc70 to synaptic plasma membrane, but also maintains high levels of Hsc70 associated with SVs. Interestingly, Hsc70 binds to CSP, another SV-associated protein, which could provide a targeting cue for Hsc70 as well as CHL1. Although levels of Hsc70 associated with SVs were not found to be abnormal in CSP-deficient

mice (Tobaben et al., 2001), binding of Hsc70 to CSP, the levels of which are strongly increased in *CHL1*$^{-/-}$ SVs, may explain the rather mild phenotype of *CHL1*$^{-/-}$ mice and residual targeting of endogenous or overexpressed Hsc70 to synapses in the absence of CHL1.

Reduced uptake and rate of release of FM dyes from *CHL1*$^{-/-}$ synapses suggest that SV recycling is slowed down in *CHL1*$^{-/-}$ mice. It is likely that reduced rate of clathrin coat release from CCSVs results in slower processing of SVs via the recycling pathway. In addition, slowed recycling rates may reflect the lack of availability of essential coat proteins to form new CCSVs in an activity-dependent manner: clathrin, AP180, and AP2 could be trapped in CCSVs formed during previous cycles of neuronal activity, and would thus be unavailable to form new CCSVs. This hypothesis is supported by our observation that, while *CHL1*$^{-/-}$ synaptic boutons accumulate abnormally high numbers of CCSVs under conditions of spontaneous activity in cultured hippocampal neurons, formation of new CCSVs in *CHL1*$^{-/-}$ synaptic boutons in response to a new stimulus, such as high K^+ application, is inhibited.

Besides regulating uncoating of CCSVs, Hsc70 also plays a role in SV exocytosis in cooperation with CSP (Bronk et al., 2001). Normal SV exocytosis in *CHL1*$^{-/-}$ mice may be related to increased levels of CSP and Hsp70, which may partially compensate for abnormal Hsc70 function. It is interesting in this respect that when the CHL1/Hsc70 complex is acutely disrupted in neurons by an interfering peptide, a smaller reduction in the number of SVs in response to high K^+ is observed, suggesting that fewer SVs fuse with the plasma membrane.

A reduced rate of SV recycling may affect proper functioning of neural circuits and information processing in the brain, manifested by multiple abnormalities in behavior in *CHL1*$^{-/-}$ mice. Two independent studies have shown a positive correlation between a missense polymorphism in the CHL1 gene and schizophrenia in humans (Chen et al., 2005; Sakurai et al., 2002), a finding that can not be explained by a molecular mechanism so far. Whereas an understanding of the many molecular mechanisms underlying schizophrenia remains presently rudimentary, it is well established that schizophrenia is a complex and predominantly genetic disorder. It is not characterized by a single causative gene; alterations in different critical genes predispose a subject in various ways, but in a convergent fashion, to a central pathophysiological process: an alteration in synapse function and an eventual disruption of neural circuits (Harrison and Weinberger, 2005). In this respect, it is interesting that alterations in at least one other gene, Epsin 4, encoding the clathrin-associated protein enthoprotin, also cause genetic susceptibility to schizophrenia (Pimm et al., 2005). Furthermore, expression levels of Hsc70 were also changed in animal models of schizophrenia (Fatemi et al., 2005), suggesting that abnormalities in Hsc70 function and clathrin recycling pathways may contribute to an aspect of schizophrenia etiology. Additional analyses are required to establish the mechanisms by which mutations in CHL1, and alterations in clathrin-dependent SV recycling, contribute to abnormalities in information processing in the brain that eventually result in neurological disorders.

Experimental Procedures

Antibodies and Toxins

Rabbit polyclonal antibodies against the extracellular domain of mouse CHL1 (Buhusi et al., 2003) and rat monoclonal antibody 555 against the extracellular domain of L1 (Appel et al., 1993) have been described. Mouse monoclonal antibodies against SV2 and the α1 subunit of Na,K-ATPase (α6F) (Developmental Studies Hybridoma Bank, Iowa City, IA); mouse monoclonal antibodies against the clathrin heavy chain, γ-adaptin, CSP, and EEA1 (BD Biosciences, San Jose, CA); goat polyclonal antibodies against synaptophysin, Hsp70, and Hsc70 (Santa Cruz Biotechnology, Santa Cruz, CA); mouse monoclonal antibodies against PSD95 (Upstate Biotechnology, Lake Placid, NY); rabbit polyclonal antibodies against His6 tag (Cell Signaling Technology, Inc., Beverly, MA); mouse monoclonal antibodies against MAP2; rabbit polyclonal antibodies against actin; and nonspecific rabbit Ig (Sigma, St. Louis, MO) were used after confirming that the antigen-specific antibodies reacted by western blot analysis only with bands of the correct molecular weights from mouse tissue. Rabbit polyclonal antibodies against synaptophysin and CSP were generous gifts from Reinhard Jahn (Max-Planck-Institute for Biophysics, Göttingen, Germany) and Guido Meyer (Max-Planck-Institute for Experimental Medicine, Göttingen, Germany). Secondary antibodies against rabbit, goat, rat, and mouse Ig coupled to horseradish peroxidase (HRP), Cy2, Cy3, or Cy5 were from Dianova (Hamburg, Germany). DL-AP5 and 6-cyano-7-nitroquinoxaline-2,3-dione (CNQX) were purchased from Tocris (Ballwin, MO).

Cultures and Transfection of Hippocampal Neurons and CHO Cells

Cultures of hippocampal neurons were prepared using 1- to 3-day-old *CHL1*$^{+/+}$ and *CHL1*$^{-/-}$ mice (Montag-Sallaz et al., 2002) as described (Sytnyk et al., 2002). Neurons were maintained in culture for 12–16 days. CHO cells were maintained in Glasgow-modified Eagle's medium containing 10% fetal calf serum. Hippocampal neurons were transfected 3 days after plating using Lipofectamine 2000 (GIBCO Invitrogen, Carlsbad, CA) according to the manufacturer's instructions. Peptides were introduced to neurons 12 days after plating using Chariot (Active Motif, Rixensart, Belgium) or Pulsin (Biomol, Hamburg, Germany) according to the manufacturers' instructions. Both reagents provided similar results. CHO cells were transfected using Lipofectamine with Plus reagent (GIBCO Invitrogen) following the manufacturer's instructions.

Immunofluorescence and FM Uptake Quantification

In fixed and permeabilized neurons, labeling with synaptophysin or SV2 antibodies was used to identify synaptic boutons. In live neurons, synaptic boutons were identified using FM dye labeling. In all these cases, a synaptic bouton was defined as an accumulation of the corresponding labeling with a mean intensity of at least 30% higher than background. The background was defined as the mean intensity of pixels in the square 30 × 30 pixel area located in the vicinity of the synaptic bouton in the part of the image free of synaptic boutons. Synaptic boutons were outlined using a threshold function of Scion Image software (Scion Corporation, Frederick, MD). Within the outlines, mean intensities of the labeling with the antibodies indicated in the text or with FM dyes were measured and expressed in arbitrary units, defined as 8 bit pixel values of the gray-scale image. In each experiment, images were acquired using identical settings and the same threshold was used for all groups. All experiments were performed 3–4 times with the same effect.

Clathrin Uncoating Assay

A suspension of CCSVs (25 μl) was mixed with 20 mM HEPES (pH 7.0), containing 25 mM KCl, 2 mM $MgCl_2$, 10 mM $(NH_4)_2SO_4$, 2 mM ATP, 5 mM phosphocreatine, and 5 units/ml creatine phosphokinase (Sigma) on ice. High concentrations of free K^+ ions in the uncoating buffer are required to stimulate uncoating activity of Hsc70 (Palleros et al., 1993). Samples were then incubated for 1, 3, 6, 9, 12, or 15 min at 25°C to induce clathrin uncoating. Samples were then placed on ice to stop the reaction and centrifuged at 100,000 × g for 15 min at 4°C. Supernatants containing clathrin released from the CCSVs

were collected and assayed for the amount of clathrin by western blot analysis.

Coimmunoprecipitation

Homogenates from adult mouse brains were prepared in 50 mM Tris-HCl buffer (pH 7.5) containing 1 mM of $CaCl_2$, 1 mM $MgCl_2$, and 1 mM $NaHCO_3$. Samples containing 1 mg of total protein were lysed for 40 min at +4°C with lysis buffer (pH 7.5) containing 50 mM Tris•HCl, 150 mM NaCl, 1% Nonidet P-40, 1 mM $Na_2P_2O_7$, 1 mM NaF, 1 mM EDTA, 2 mM $NaVO_4$, 0.1 mM PMSF, and complete protease inhibitor cocktail (Roche Diagnostics), and centrifuged for 15 min at 20,000 × g at 4°C. Supernatants were cleared with protein A/G-agarose beads (Santa Cruz Biotechnology) (3 hr at 4°C) and incubated with corresponding antibodies or nonspecific control Ig (overnight, 4°C), followed by precipitation with protein A/G-agarose beads (1 hr, 4°C). The beads were washed three times with lysis buffer and two times with PBS. To quantify levels of coimmunoprecipitated complexes, proteins in the same amount of starting material as used for coimmunoprecipitation, and proteins in the material that did not bind to the beads during coimmunoprecipitation, were precipitated by TCA (12.5% final concentration). Beads and precipitated proteins were boiled in the same volumes of Laemmli buffer and used for western blot analysis. Equal volumes of the samples were applied to the gels.

Supplemental Data

The Supplemental Data for this article contain details on 2D gel electrophoresis and overlay assay; DNA constructs; indirect immunofluorescence staining; analysis of CHL1 antibody uptake; loading and unloading of FM dyes; preparation of brain tissue homogenates and isolation of synaptosomes, SVs, and CCSVs; analysis of Hsc70 binding to synaptic membranes; western blot analysis; electron microscopy; and quantitative real-time PCR. They can be found online at http://www.neuron.org/cgi/content/full/52/6/1011/DC1/.

Acknowledgments

We are grateful to Drs. Bernhard Kuster and Matthias Mann (University of Southern Denmark, Odense M, Denmark) for the protein sequencing. We thank Dr. Hidde L. Ploegh (Harvard Medical School, Boston, MA, USA) for the Hsc70GFP construct, Drs. Reinhard Jahn and Guido Meyer for antibodies against synaptophysin and CSP, and Drs. Christine Knuehl, Jaewhan Song, and Guido Meyer for constructs encoding Hsc70, BAG-1, and CSP for bacterial production. We are also grateful to Ute Eicke-Kohlmorgen, Achim Dahlmann, and Eva Kronberg for technical assistance, genotyping, and animal care. This work was supported by Zonta Club, Hamburg-Alster (I.L.) and Deutsche Forschungsgemeinschaft (M.S.).

Received: February 10, 2006
Revised: August 17, 2006
Accepted: October 20, 2006
Published: December 20, 2006

References

Ahmari, S.E., Buchanan, J., and Smith, S.J. (2000). Assembly of presynaptic active zones from cytoplasmic transport packets. Nat. Neurosci. *3*, 445–451.

Angeloni, D., Wei, M.H., and Lerman, M.I. (1999a). Two single nucleotide polymorphisms (SNPs) in the CALL gene for association studies with IQ. Psychiatr. Genet. *9*, 165–167.

Angeloni, D., Lindor, N.M., Pack, S., Latif, F., Wei, M.H., and Lerman, M.I. (1999b). CALL gene is haploinsufficient in a 3p- syndrome patient. Am. J. Med. Genet. *86*, 482–485.

Appel, F., Holm, J., Conscience, J.F., and Schachner, M. (1993). Several extracellular domains of the neural cell adhesion molecule L1 are involved in neurite outgrowth and cell body adhesion. J. Neurosci. *13*, 4764–4775.

Bloom, O., Evergren, E., Tomilin, N., Kjaerulff, O., Low, P., Brodin, L., Pieribone, V.A., Greengard, P., and Shupliakov, O. (2003). Colocalization of synapsin and actin during synaptic vesicle recycling. J. Cell Biol. *161*, 737–747.

Bronk, P., Wenniger, J.J., Dawson-Scully, K., Guo, X., Hong, S., Atwood, H.L., and Zinsmaier, K.E. (2001). Drosophila Hsc70-4 is critical for neurotransmitter exocytosis in vivo. Neuron *30*, 475–488.

Buhusi, M., Midkiff, B.R., Gates, A.M., Richter, M., Schachner, M., and Maness, P.F. (2003). Close homolog of L1 is an enhancer of integrin-mediated cell migration. J. Biol. Chem. *278*, 25024–25031.

Carroll, R.C., Beattie, E.C., Xia, H., Luscher, C., Altschuler, Y., Nicoll, R.A., Malenka, R.C., and von Zastrow, M. (1999). Dynamin-dependent endocytosis of ionotropic glutamate receptors. Proc. Natl. Acad. Sci. USA *96*, 14112–14117.

Carter, L.L., Redelmeier, T.E., Woollenweber, L.A., and Schmid, S.L. (1993). Multiple GTP-binding proteins participate in clathrin-coated vesicle-mediated endocytosis. J. Cell Biol. *120*, 37–45.

Chamberlain, L.H., and Burgoyne, R.D. (1997). The molecular chaperone function of the secretory vesicle cysteine string proteins. J. Biol. Chem. *272*, 31420–31426.

Chang, H.C., Newmyer, S.L., Hull, M.J., Ebersold, M., Schmid, S.L., and Mellman, I. (2002). Hsc70 is required for endocytosis and clathrin function in Drosophila. J. Cell Biol. *159*, 477–487.

Chen, Q.Y., Chen, Q., Feng, G.Y., Lindpaintner, K., Chen, Y., Sun, X., Chen, Z., Gao, Z., Tang, J., and He, L. (2005). Case-control association study of the close homologue of L1 (CHL1) gene and schizophrenia in the Chinese population. Schizophr. Res. *73*, 269–274.

Demyanenko, G.P., Schachner, M., Anton, E., Schmid, R., Feng, G., Sanes, J., and Maness, P.F. (2004). Close homolog of L1 modulates area-specific neuronal positioning and dendrite orientation in the cerebral cortex. Neuron *44*, 423–437.

Fatemi, S.H., Pearce, D.A., Brooks, A.I., and Sidwell, R.W. (2005). Prenatal viral infection in mouse causes differential expression of genes in brains of mouse progeny: a potential animal model for schizophrenia and autism. Synapse *57*, 91–99.

Frints, S.G., Marynen, P., Hartmann, D., Fryns, J.P., Steyaert, J., Schachner, M., Rolf, B., Craessaerts, K., Snellinx, A., Hollanders, K., et al. (2003). CALL interrupted in a patient with non-specific mental retardation: gene dosage-dependent alteration of murine brain development and behavior. Hum. Mol. Genet. *12*, 1463–1474.

Gerrow, K., and El-Husseini, A. (2006). Cell adhesion molecules at the synapse. Front. Biosci. *11*, 2400–2419.

Hannah, M.J., Schmidt, A.A., and Huttner, W.B. (1999). Synaptic vesicle biogenesis. Annu. Rev. Cell Dev. Biol. *15*, 733–798.

Harata, N., Pyle, J.L., Aravanis, A.M., Mozhayeva, M., Kavalali, E.T., and Tsien, R.W. (2001). Limited numbers of recycling vesicles in small CNS nerve terminals: implications for neural signaling and vesicular cycling. Trends Neurosci. *24*, 637–643.

Harrison, P.J., and Weinberger, D.R. (2005). Schizophrenia genes, gene expression, and neuropathology: on the matter of their convergence. Mol. Psychiatry *10*, 40–68.

Hillenbrand, R., Molthagen, M., Montag, D., and Schachner, M. (1999). The close homologue of the neural adhesion molecule L1 (CHL1): patterns of expression and promotion of neurite outgrowth by heterophilic interactions. Eur. J. Neurosci. *3*, 813–826.

Irintchev, A., Koch, M., Needham, L.K., Maness, P., and Schachner, M. (2004). Impairment of sensorimotor gating in mice deficient in the cell adhesion molecule L1 or its close homologue, CHL1. Brain Res. *1029*, 131–134.

Mahaffey, D.T., Moore, M.S., Brodsky, F.M., and Anderson, R.G. (1989). Coat proteins isolated from clathrin coated vesicles can assemble into coated pits. J. Cell Biol. *108*, 1615–1624.

Massol, R.H., Boll, W., Griffin, A.M., and Kirchhausen, T. (2006). A burst of auxilin recruitment determines the onset of clathrin-coated vesicle uncoating. Proc. Natl. Acad. Sci. USA *103*, 10265–10270.

Maycox, P.R., Link, E., Reetz, A., Morris, S.A., and Jahn, R. (1992). Clathrin-coated vesicles in nervous tissue are involved primarily in synaptic vesicle recycling. J. Cell Biol. *118*, 1379–1388.

Montag-Sallaz, M., Schachner, M., and Montag, D. (2002). Misguided axonal projections, neural cell adhesion molecule 180 mRNA upregulation, and altered behavior in mice deficient for the close homolog of L1. Mol. Cell. Biol. *22*, 7967–7981.

Morgan, J.R., Prasad, K., Jin, S., Augustine, G.J., and Lafer, E.M. (2001). Uncoating of clathrin-coated vesicles in presynaptic terminals: roles for Hsc70 and auxilin. Neuron *32*, 289–300.

Newmyer, S.L., and Schmid, S.L. (2001). Dominant-interfering Hsc70 mutants disrupt multiple stages of the clathrin-coated vesicle cycle in vivo. J. Cell Biol. *152*, 607–620.

Nikonenko, A.G., Sun, M., Lepsveridze, E., Apostolova, I., Petrova, I., Irintchev, A., Dityatev, A., and Schachner, M. (2006). Enhanced perisomatic inhibition and impaired long-term potentiation in the CA1 region of juvenile CHL1-deficient mice. Eur. J. Neurosci. *23*, 1839–1852.

Palleros, D.R., Reid, K.L., Shi, L., Welch, W.J., and Fink, A.L. (1993). ATP-induced protein-Hsp70 complex dissociation requires K^+ but not ATP hydrolysis. Nature *365*, 664–666.

Pimm, J., McQuillin, A., Thirumalai, S., Lawrence, J., Quested, D., Bass, N., Lamb, G., Moorey, H., Datta, S.R., Kalsi, G., et al. (2005). The Epsin 4 gene on chromosome 5q, which encodes the clathrin-associated protein enthoprotin, is involved in the genetic susceptibility to schizophrenia. Am. J. Hum. Genet. *76*, 902–907.

Pratte, M., Rougon, G., Schachner, M., and Jamon, M. (2003). Mice deficient for the close homologue of the neural adhesion cell L1 (CHL1) display alterations in emotional reactivity and motor coordination. Behav. Brain Res. *147*, 31–39.

Richards, D.A., Guatimosim, C., and Betz, W.J. (2000). Two endocytic recycling routes selectively fill two vesicle pools in frog motor nerve terminals. Neuron *27*, 551–559.

Rizzoli, S.O., and Betz, W.J. (2005). Synaptic vesicle pools. Nat. Rev. Neurosci. *6*, 57–69.

Sakurai, K., Migita, O., Toru, M., and Arinami, T. (2002). An association between a missense polymorphism in the close homologue of L1 (CHL1, CALL) gene and schizophrenia. Mol. Psychiatry *7*, 412–415.

Schmid, S.L., and Smythe, E. (1991). Stage-specific assays for coated pit formation and coated vesicle budding in vitro. J. Cell Biol. *114*, 869–880.

Schmid, S.L. (1997). Clathrin-coated vesicle formation and protein sorting: an integrated process. Annu. Rev. Biochem. *66*, 511–548.

Shupliakov, O., Low, P., Grabs, D., Gad, H., Chen, H., David, C., Takei, K., De Camilli, P., and Brodin, L. (1997). Synaptic vesicle endocytosis impaired by disruption of dynamin-SH3 domain interactions. Science *276*, 259–263.

Smythe, E., Pypaert, M., Lucocq, J., and Warren, G. (1989). Formation of coated vesicles from coated pits in broken A431 cells. J. Cell Biol. *108*, 843–853.

Sollner, T., Bennett, M.K., Whiteheart, S.W., Scheller, R.H., and Rothman, J.E. (1993). A protein assembly-disassembly pathway in vitro that may correspond to sequential steps of synaptic vesicle docking, activation, and fusion. Cell *75*, 409–418.

Sytnyk, V., Leshchyns'ka, I., Delling, M., Dityateva, G., Dityatev, A., and Schachner, M. (2002). Neural cell adhesion molecule promotes accumulation of TGN organelles at sites of neuron-to-neuron contacts. J. Cell Biol. *159*, 649–661.

Sytnyk, V., Leshchyns'ka, I., Dityatev, A., and Schachner, M. (2004). Trans-Golgi network delivery of synaptic proteins in synaptogenesis. J. Cell Sci. *117*, 381–388.

Takayama, S., Xie, Z., and Reed, J.C. (1999). An evolutionarily conserved family of Hsp70/Hsc70 molecular chaperone regulators. J. Biol. Chem. *274*, 781–786.

Takei, K., Mundigl, O., Daniell, L., and De Camilli, P. (1996). The synaptic vesicle cycle: a single vesicle budding step involving clathrin and dynamin. J. Cell Biol. *133*, 1237–1250.

Tobaben, S., Thakur, P., Fernandez-Chacon, R., Sudhof, T.C., Rettig, J., and Stahl, B. (2001). A trimeric protein complex functions as a synaptic chaperone machine. Neuron *31*, 987–999.

Tsai, J., and Douglas, M.G. (1996). A conserved HPD sequence of the J-domain is necessary for YDJ1 stimulation of Hsp70 ATPase activity at a site distinct from substrate binding. J. Biol. Chem. *271*, 9347–9354.

Virmani, T., Han, W., Liu, X., Sudhof, T.C., and Kavalali, E.T. (2003). Synaptotagmin 7 splice variants differentially regulate synaptic vesicle recycling. EMBO J. *22*, 5347–5357.

Yao, P.J., Coleman, P.D., and Calkins, D.J. (2002). High-resolution localization of clathrin assembly protein AP180 in the presynaptic terminals of mammalian neurons. J. Comp. Neurol. *447*, 152–162.

Zhai, R.G., Vardinon-Friedman, H., Cases-Langhoff, C., Becker, B., Gundelfinger, E.D., Ziv, N.E., and Garner, C.C. (2001). Assembling the presynaptic active zone: a characterization of an active one precursor vesicle. Neuron *29*, 131–143.

Zinsmaier, K.E., and Bronk, P. (2001). Molecular chaperones and the regulation of neurotransmitter exocytosis. Biochem. Pharmacol. *62*, 1–11.